British Journal of Pharmacology (2005) 144, 743–754
www.nature.com/bjp

Functional implications of modifying RyR-activating peptides for membrane permeability

*,[1]Angela F. Dulhunty, [1]Louise Cengia, [1]Jacqui Young, [1]Suzy M. Pace, [1]Peta J. Harvey, [1,2]Graham D. Lamb, [1,3]Yiu-Ngok Chan, [1,3]Norbert Wimmer, [1,3]Istvan Toth & [1]Marco G. Casarotto

[1]Division of Molecular Bioscience, John Curtin School of Medical Research, Australian National University, PO Box 334, Canberra, ACT 2601, Australia; [2]The Department of Zoology, La Trobe University, Bundoora, Victoria, Australia and [3]The School of Pharmacy, University of Queensland, Brisbane, Australia

1 Our aim was to determine whether lipoamino acid conjugation of peptides that are high-affinity activators of ryanodine receptor (RyR) channels would (a) render the peptides membrane permeable, (b) alter their structure or (a) reduce their activity. The peptides correspond to the ***A*** region of the II–III loop of the skeletal dihydropyridine receptor.

2 The lipoamino acid conjugation increased the apparent permeability of the peptide across the Caco-2 cell monolayer by up to ~20-fold.

3 Nuclear magnetic resonance showed that the α-helical structure of critical basic residues, required for optimal activation of RyRs, was retained after conjugation.

4 The conjugated peptides were more effective in enhancing resting Ca^{2+} release, Ca^{2+}-induced Ca^{2+} release and caffeine-induced Ca^{2+} release from isolated sarcoplasmic reticulum (SR) than their unconjugated counterparts, and significantly enhanced caffeine-induced Ca^{2+} release from mechanically skinned extensor digitorum longus (EDL) fibres.

5 The effect of both conjugated and unconjugated peptides on Ca^{2+} release from skeletal SR was 30-fold greater than their effect on either cardiac Ca^{2+} release or on the Ca^{2+} Mg^{2+} ATPase.

6 A small and very low affinity effect of the peptide in slowing Ca^{2+} uptake by the Ca^{2+}, Mg^{2+} ATPase was exacerbated by lipoamino acid conjugation in both isolated SR and in skinned EDL fibres.

7 The results show that lipoamino acid conjugation of ***A*** region peptides increases their membrane permeability without impairing their structure or efficacy in activating skeletal and cardiac RyRs.
British Journal of Pharmacology (2005) **144,** 743–754. doi:10.1038/sj.bjp.0705981
Published online 13 December 2004

Keywords: Lipoamino acid conjugation; ryanodine receptor; sarcoplasmic reticulum; skeletal muscle; cardiac muscle; Ca^{2+} release

Abbreviations: Caco-2, human colon carcinoma epithelial cell line; CICR, calcium-induced calcium release; DHPR, dihydropyridine receptor; EC coupling, excitation–contraction coupling; EDL, extensor digitorum longus; HBSS, Hanks' balanced salt solution; LC–MS, liquid chromatography–mass spectrometry; LHRH, luteinising hormone-releasing hormone; II–III loop, loop between the second and third membrane-spanning segment of the DHPR; P_{app}, apparent permeability coefficient; RyR, ryanodine receptor; SR, sarcoplasmic reticulum; TEER, *trans*-epithelial electrical resistance

Introduction

The ryanodine receptor (RyR) Ca^{2+} release channel is the sole conduit for Ca^{2+} release from internal stores in the sarcoplasmic reticulum (SR) to activate contraction in skeletal muscle and the heart. The RyR, either alone or in combination with the inositol 1,4,5-trisphosphate receptor (IP_3R), is also found in the endoplasmic reticulum, mitochondria, nuclear envelope and secretory vesicles of many cell types, including smooth muscle, neurones and lymphocytes. Despite the importance of this ion channel, there are few drugs available that can be used either as experimental probes for RyR activity or for therapeutic purposes.

A 20 amino-acid peptide (peptide ***A***), corresponding to a part of the loop between the second and third membrane-spanning segment of the skeletal dihydropyridine receptor (DHPR), is a part of a naturally occurring muscle protein and is a high-affinity activator of skeletal and cardiac RyR channels (El-Hayek *et al*., 1995; Dulhunty *et al*., 1999; Gurrola *et al*., 1999; Lamb *et al*., 2000; Stange *et al*., 2001; Dulhunty *et al*., 2002). Both the DHPR and the RyR are essential for skeletal muscle contraction (Tanabe *et al*., 1988). A strict alignment (Block *et al*., 1988) allows physical coupling between the II–III loop of the DHPR and the RyR to initiate skeletal-type excitation–contraction (EC) coupling (which is independent of external Ca^{2+}). Although the ***A*** region of the II–III loop is not required for EC coupling (Proenza *et al*., 2000; Wilkens *et al*., 2001), it has been implicated in the overall physical interaction between the DHPR and RyR (Ahern *et al*., 2001).

*Author for correspondence; E-mail: angela.dulhunty@anu.edu.au
Published online 13 December 2004

A sequence of positively charged residues (El-Hayek *et al*., 1995; Gurrola *et al*., 1999; Casarotto *et al*., 2000, 2001), and the alignment of the residues along one surface of the molecule (Casarotto *et al*., 2000; 2001; Green *et al*., 2003), are critical for peptide ***A*** to activate RyR channels. Modified ***A*** peptides having the most stable α-helical structure are the strongest activators of the RyR and have a surface orientation of positively charged residues similar to that in two scorpion toxins, Imperatoxin A and Maurocalcine (Mosbah *et al*., 2000; Green *et al*., 2003). The toxins, like the peptide, are high-affinity activators of the RyR and thought to bind to a similar site on the RyR (Tripathy *et al*., 1998; Gurrola *et al*., 1999; Green *et al*., 2003). The ***A*** peptides are potentially useful as probes for RyR channel activity and would be more useful if they could be modified for membrane permeability without loss of function.

In this study, we have made the ***A*** peptides membrane permeable by conjugating them to C_{12} or C_{10} lipoamino acids, to alter their physico-chemical properties. Lipoamino acids are α amino acids with long alkyl side-chains, which can enhance the membrane permeability, intestinal absorption and metabolic stability of peptides and have been investigated extensively in drug delivery (Toth *et al*., 1999; Toth & Keri, 2003). We have assessed the permeability of the lipoamino acid-conjugated ***A*** peptides, examined their structure and assessed their ability to release Ca^{2+} from cardiac and skeletal SR vesicles and from the SR in skinned skeletal muscle fibres. The results show that the lipid modification of the ***A*** peptides (a) increased their permeability, (b) did not significantly alter their structure, (c) enhanced their ability to activate Ca^{2+} release from isolated SR, (d) did not significantly alter their ability to activate the RyR in skinned muscle fibres and (e) enhanced a lower-affinity action of the peptide on Ca^{2+} uptake by the Ca^{2+}, Mg^{2+} ATPase in the SR.

Methods

Peptides and peptide synthesis

The ***A***-series peptides, ***A1***, ***A2***, ***A1(D-R18)*** and ***A2(D-R18)*** (Table 1) were synthesised by the JCSMR Biomolecular Resource Facility using an Applied Biosystems 430A Peptide Synthesiser with purification to 98–100% using HPLC and mass spectroscopy. Stock peptide solutions (~2 mM) were prepared in H_2O and frozen in 20 μl aliquots (Dulhunty *et al*., 1999).

Lipid conjugation

Lipoamino acids, α-aminodecanoic acid and α-aminododecanoic acid were synthesised (Gibbons *et al*., 1990), purified, triturated with acetonitrile, then re-crystallised. The α-aminodecanoic acid was coupled to the resin once (or twice), then coupled to peptide ***A2 (D-R18)*** to yield ***A2(D-R18)-C10*** (or ***A2(D-R18)-2C10***). Likewise, α-aminododecanoic acid was coupled once to ***A2(D-R18)*** to obtain ***A2(D-R18)-C12***. Sequences of ***A2*** and ***A2(D-R18)*** and the lipoamino acid structures are:

A2 = TSAQKAKAEERKRRKMARGL

A2(D-R18) = TSAQKAKAEERKRRKMA(D-R)GL

A2(D-R18)-C10

A2(D-R18)-2C10

A2(D-R18)-*C12*

where ***-C10*** ***-2C10*** ***-C12***

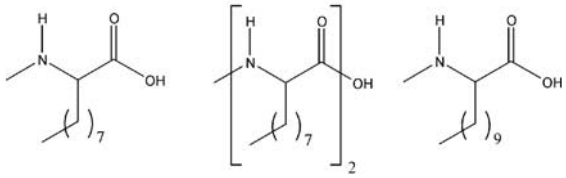

Membrane permeability assessment

Caco-2 (human colon carcinoma; American Type Culture Collection) epithelial cell lines were cultivated as monolayers on permeable filters (Artursson & Karlsson, 1991). The cells were maintained in tissue culture flasks (Nunc, Roskilde, Denmark) and seeded at $\sim 5 \times 10^5$ cells cm^{-2} into 6.5 mm Transwells® with polycarbonate membranes (0.4 μm pore, Costar, Cambridge, U.S.A.). The culture medium (Dulbecco's modified Eagle's medium, Gibco Paisley, Scotland) was supplemented with 10% foetal calf serum, 1% nonessential amino acids, 1% L-glutamine and 1% penicillin and streptomycin. The media was replaced every 48 h, with 0.1 ml on the apical side and 0.6 ml on the basolateral side. Cells with a passage number of 55 were used in experiments. The integrity of the monolayers was monitored by the transepithelial electrical resistance (TEER) and mannitol permeability.

Apparent permeability

At 30 days after seeding, the cells were washed and equilibrated in Hanks' balanced salt solution (HBSS) at 37°C on apical and basolateral sides. The cells were placed in new wells containing 0.6 ml of HBSS. In all, 200 μM of test compound was added to the apical side and the inserts transferred to new wells every 30 min over 3 h. Concentrations of test compounds in the basolateral solution were determined by liquid chromatography–mass spectrometry (LC–MS). The apparent permeability coefficient P_{app} (cm s^{-1}) was calculated as:

$$P_{app} = (\Delta Q/\Delta t)/AC_0$$

where $\Delta Q/\Delta t$ is the permeability rate, A is the surface area of the monolayer and C_0 is the initial concentration of the peptide on the apical side. The mannitol permeability assay was performed using D-Mannitol-1-^{14}C, (Sigma) as described previously (Artursson *et al*., 2001).

Electrical measurements

TEER was measured at 37°C with a Millicell-electrical resistance system (ERS). The Caco-2 monolayers were incubated for 30 min, and the electrodes equilibrated for 15 min, in HBBS before TEER measurements 1 day and 30 min before, and immediately after, the experiment. The filter resistance without the cells (4–5 Ω cm^2) was subtracted from TEER values.

LC/MS analysis

A Perkin-Elmer Sciex API 3000 combined with Shimadzu HPLC was used to detect and measure peptides. A volume of 10 μl of HBBS/peptide sample was injected into the LC/MS. An Agilent C18 column (Zorbax 5 μm SB-C18 2.1 × 50 mm^2) with C18 guard column and 1 : 10 splitter was used. Mobile phase A was 0.1% formic acid in H_2O; B was 90% acetonitrile with 0.1% formic acid. The solvent gradient was started with 0% B for 0.6 min, increased to 100% B at 1.6 min, retained for 1.9 min and decreased to 0% B in 0.1 min at a constant flow of 0.2 ml min^{-1}. Standards were prepared from 0.001 to 5 μM. Standard curves achieved $R^2 > 0.999$.

Nuclear magnetic resonance (NMR) spectroscopy

Peptides ***A2(D-R18)***, ***A2(D-R18)-2C$_{10}$*** and ***A2(D-R18)-C$_{12}$*** were dissolved in 10% D_2O/90% H_2O to a final concentration of ~2 mM at pH ~5.5. NMR spectroscopy and subsequent analysis were then performed as described previously (Casarotto *et al*., 2000; 2001).

Isolation of SR vesicles

Skeletal SR was isolated from the back and leg muscles of New Zealand White rabbits, and heavy SR was collected from the 35–45% (w v^{-1}) interface of a discontinuous sucrose gradient, centrifuged and resuspended (Ahern *et al*., 1994). Cardiac SR was prepared from sheep heart (Chamberlain & Fleischer, 1988; Laver *et al*., 1995). Vesicles were frozen and stored either in liquid N_2 or at −70°C.

Ca^{2+} release

Extravesicular Ca^{2+} was monitored at 710 nm with the Ca^{2+} indicator, antipyrylazo III, using a Cary 3 spectrophotometer (Dulhunty *et al*., 1999). Identical release experiments were performed at 790 nm, to detect Ca^{2+}-independent changes in optical density (OD), which would alter the Ca^{2+} release measurement. The cuvette solution was stirred continuously and temperature controlled at 25°C. A typical Ca^{2+}-release experiment is shown in Figure 3. Skeletal SR (100 μg of protein) was added to the cuvette solution (final volume of 2 ml), containing (mM): KH_2PO_4, 100 (pH = 7); $MgCl_2$, 4; Na_2ATP, 1; antipyrylazo III, 0.5). Ca^{2+}, Mg^{2+}-ATPase activity was suppressed with thapsigargin (200 nM; Sagara & Inesi, 1991). The same solutions were used with cardiac SR, except that an ATP-regenerating system – phospho(enol)pyruvate (5 mM) and pyruvate kinase (25 μg ml^{-1}) – was added. OD calibration curves were obtained daily. The same conditions were used for Ca^{2+} accumulation experiments, except that the concentration of antipyrylazo III was 0.2 mM. Control experiments, performed either without SR vesicles or when the SR vesicles were blocked with thapsigargin, ruthenium red and ionophore, showed that addition of the **-2C10** conjugated peptides elicited a step change in OD and then a slow increase. This artefactual change in OD was similar for all **-2C10** conjugated peptides, and increased with peptide concentration from negligible levels at ⩽1 μM peptide to values equivalent to Ca^{2+} release rates of ~5 ± 3 and 64 ± 10 nmol mg^{-1} min^{-1} at 5 and 30 μM peptide, respectively. Measurements of Ca^{2+}-release rate obtained in experiments where **-2C10** conjugated peptide was added to Ca^{2+}-loaded vesicles were corrected for this artefact by subtracting the appropriate value. It was possible that this intrinsic optical effect was due to an isomer ***A2(D-R18)-2C$_{10}$***. The peptide ***A2(D-R18)*** is made with optically pure L-amino acids and D-R18. The lipoamino acid (C_{10}) was a racemate (L-C_{10} and D-C_{10}), so that one C_{10} conjugation gave two diastereomers and the second coupling gave four diastereomers. These diastereomers were separated by HPLC and two major fractions obtained. Fraction 1 produced much less artefactual change in OD but retained its efficacy in activating Ca^{2+} release, while fraction 4 had less functional activity and produced a strong artefactual response.

Skinned fibre techniques

Experiments were performed at 23 ± 2°C and chemicals obtained from Sigma, except where noted. Mechanically skinned segments of single extensor digitorum longus (EDL) muscle fibres from the rat were connected to a force transducer (AME801, SensoNor, Horten, Norway), and bathed in a standard high [K^+] solution mimicking the normal environment (Lamb & Stephenson, 1994) and containing (mM): K^+, 126; Na^+, 37; 1,6-diaminohexane-*N*,*N*,*N*′,*N*′-tetraacetic acid (HDTA) (Fluka, Buchs, Switzerland), 50; total ATP, 8.0; total creatine phosphate, 10.0; total magnesium, 8.5; HEPES, 90; NaN_3, 1.0; total EGTA, 0.05, with pCa (i.e. $-\log_{10}[Ca^{2+}]$) 7.1 and pH 7.10 ± 0.01 (free [Mg^{2+}], 1 mM; osmolality, 295 ± 5 mosmol kg^{-1}). The SR was fully emptied of Ca^{2+} by pre-equilibrating the fibre in standard solution with 0.5 mM EGTA (pCa > 8) for 10 s and then exposing it to the Full Release Solution (similar solution with 30 mM caffeine, 0.05 mM free Mg^{2+} and 0.5 mM EGTA, pCa > 8). The time integral (area) of the force response upon emptying the SR with the Full Release Solution indicated the amount of Ca^{2+} present in the SR (Lamb *et al*., 2001).

To test the sensitivity to 8 mM caffeine (e.g. Figure 9), the SR was loaded with Ca^{2+} to a set level (close to that in the fibre endogenously) by exposing the fibre for a set period (usually 15 s) to a solution buffered at pCa 6.7 with 1.0 mM total EGTA (Lamb *et al*., 2001). The fibre was then equilibrated in standard weakly Ca^{2+}-buffered solution (1 mM Mg^{2+}, 0.05 mM EGTA, pCa 7.1) for 20 s, with or without peptide, and exposed to a similar solution with 8 mM caffeine for 15 s, before fully depleting the SR of its remaining Ca^{2+} with the Full Release Solution. Maximum Ca^{2+}-activated force in each fibre was determined using a 50 mM Ca-EGTA (pCa 4.7) ('Max') solution.

To examine the effect of a peptide on Ca^{2+} accumulation (Figure 10), the fibre was subjected to repeated load-deplete cycles in which the SR was loaded for a set period with peptide present or absent, and then emptied of all Ca^{2+} with the standard Full Release Solution (without peptide) to ascertain the total Ca^{2+} accumulated. When loading in standard 1 mM Mg^{2+}, the load solution was at pCa 6.7 (1 mM total EGTA), but when loading at 10 mM Mg^{2+} the free [Ca^{2+}] was increased to pCa 6.4. Before loading, the fibre was pre-equilibrated for 1 min in a solution with 0.5 mM EGTA (pCa > 8) with or without peptide. To examine the Ca^{2+} sensitivity of the contractile apparatus, a fibre was exposed to matched sequences of solutions, both with and without the peptide, in which the [Ca^{2+}] was heavily Ca^{2+}-buffered

(50 mM total EGTA replacing HDTA) at progressively higher levels (pCa 6.7–4.7) (Lamb & Stephenson, 1994). The steady-state force produced at each pCa was expressed relative to the respective maximum, and the force–pCa relationship was best fit with a Hill curve to give the pCa producing half-maximal force (pCa_{50}) and the Hill coefficient.

Statistics

Average data are given as mean ± s.e.m. for $n \geqslant 4$, or mean ± s.d. for $n = 3$. The significance of the difference between control and test values was tested using a Student's *t*-test.

Results

Membrane permeability of the peptides

The peptide sequences are shown in Table 1. The novel ***A2(D-R18)*** contained two modifications of the native ***A1*** sequence, which increase structural stability. Ser17 was mutated to an alanine (Casarotto *et al*., 2000) and the L isomer of Arg18 was replaced by the D isomer (Green *et al*., 2003). The apparent permeabilities of ***A2(D-R18)*** and ***A2(D-R18)-2C$_{10}$*** were measured and compared with a single tail of the same chain length, ***A2(D-R18)-C$_{10}$***. The amount of peptide transported across the Caco-2 cell monolayer increased with lipoamino acid conjugation (Figure 1a). The apparent permeabilities were 4.17 ± 0.5E–08 cm s^{-1} for ***A2(D-R18)***, 24.7 ± 1.46E–08 cm s^{-1} for ***A2(D-R18)-2C$_{10}$*** and 91.5 ± 6.1E–08 cm s^{-1} for the single -C_{10} conjugate.

The relatively small permeability for ***A2(D-R18)-2C$_{10}$*** was surprising, but is likely to reflect lower than expected concentrations in the donor compartment because the more hydrophobic peptide was adsorbed onto the surface of the sample well (Artursson & Karlsson, 1991). In contrast, since ***A2(D-R18)-C$_{10}$*** would have no significant plastic adsorption, its apparent permeability is a more accurate reflection of the true permeability of the tailed peptides. TEER values (Figure 1b) and the mannitol permeability assay indicated that the cells remained in good condition. TEER remained $\geqslant$30% of control in all cases. Toxicity is indicated by a fall to $<$10% of control (Ingels *et al*., 2002). A smaller fall in TEER over the experimental period with both the permeable and impermeable compounds was not indicative of toxicity. Mannitol permeability, measured in parallel with compound permeability, remained between 2.4E–07 and 2.9E–07 cm s^{-1} and well within the normal range of 1.8E–07 to 1.17E–06 (Artursson *et al*., 1996). Mannitol is restricted to the paracellular pathway across the tight junctions and its permeability indicates the tightness of the junction. The permeability will significantly increase if cells are damaged, as mannitol diffuses between the donor and the receiver compartments.

Since lipophylic compounds are excluded from paracellular pathways, it is well recognised that their permeability reflects their movement across the cell membranes, provided the cells are not damaged (Wong *et al*., 2002). Since TEER and mannitol permeability indicated that the cells in this study remained in good condition, the increase in permeability

Table 1 Effects of various A-series peptides on the initial rate of CICR from cardiac SR vesicles

	Relative release rate	
Peptide	*10* μM	*30* μM
A1 Thr Ser Ala Gln Lys Ala Lys Ala Glu Glu Arg Lys ArgArg Lys Met Ser Arg Gly Leu	2.15 ± 0.23* (4)	1.83 ± 0.15* (9)
A2 Thr Ser Ala Gln Lys Ala Lys Ala Glu Glu Arg Lys Arg Arg Lys Met **Ala** Arg Gly Leu	2.03 ± 0.03* (5)	2.61 ± 0.34* (5)
A2(D-R18) Thr Ser Ala Gln Lys Ala Lys Ala Glu Glu Arg Lys Arg Arg Lys Met **Ala** ***Arg*** Gly Leu	3.02 ± 0.50* (6)	2.77 ± 0.39* (9)
A2(D-R18)-C12	1.58 ± 0.15 (3)	0.77 ± 0.17 (3)
A2(D-R18)-2C10	2.45 ± 0.23* (3)	4.51 ± 1.12* (4)

The rate of CICR in the presence of 10 or 30 μM peptide is expressed relative to that with no added peptide (control). Number of experiments is given in brackets. The sequence for each of the peptides is given. Residues altered from the native ***A1*** sequence are highlighted. The Ser to Ala mutation in ***A2***, ***A2(D-R18)*** is shown in bold type, and L-Arg to D-Arg replacement in ***A2(D-R18)*** is shown in bold italics. **-C12** indicates that the peptide conjugated to a single **-C12** tail, while **-2C10** indicates conjugation to two **-C10** tails. Asterisks indicate that the data are significantly different from control (i.e. 1.0).

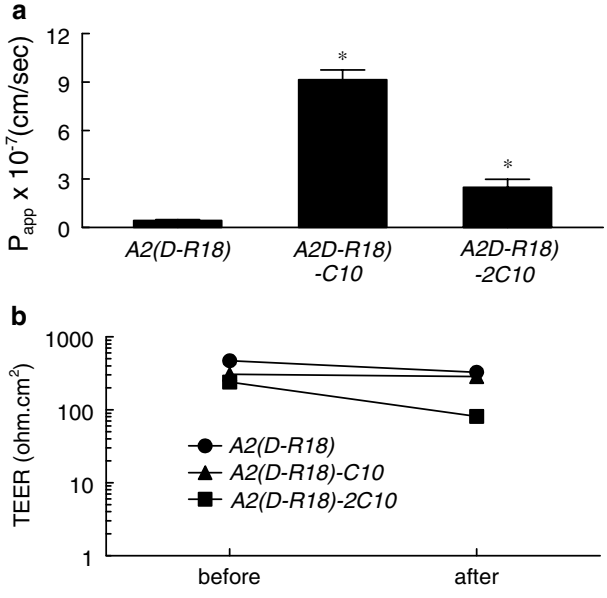

Figure 1 Conjugation of two -C10 lipid tails to ***A2(D-R18)*** allows the peptide to cross Caco-2 cell membranes. (a) The apparent permeability of Caco-2 cell monolayers for peptides ***A2(D-R18)***, ***A2(D-R18)-C10*** and ***A2(D-R18)-2C10***. Each bar show the mean ± s.d. for P_{app} obtained from three experiments. The asterisks indicate a significant difference from data obtained with ***A2(D-R18)***. (b) Average TEER measurements obtained from the monolayer before and after permeability measurements using ***A2(D-R18)*** ($n = 3$), ***A2(D-R18)-C10*** ($n = 4$) and ***A2(D-R18)-2C10*** ($n = 4$).

of the -C10 conjugates is indicative of increased membrane permeability.

Structure of A2(D-R18) *lipid-conjugated peptides*

The complete NMR assignments were determined using standard two-dimensional methods with TOSCY experiments (Bax & Davis, 1985) to identify spin types and NOESY experiments (Kumar *et al*., 1980) for specific sequence assignments. The extent of α-helical structure was assessed from NOE cross-peaks, which indicate that two proton atoms are separated by $\sim <5$ Å. Adjacent amide backbone protons in an α-helix are separated by $\sim <2.8$ Å and typical NOE patterns reflecting α-helical structure are shown in Figure 2.

The spectrum for ***A2(D-R18)*** (Figure 2a) indicates a helix extending throughout the entire peptide from residue 1 to 20, with a helical structure comparable to that in ***A1(D-R18***) (Green *et al*., 2003). Fewer NOESY cross-peaks were present in the spectrum for the active fraction 1 of ***A2(D-R18)-2C$_{10}$*** (Figure 2b). These cross-peaks, as well as the α-proton chemical shift, indicate a helical structure between residues 2 and 15 (Casarotto *et al*., 2001). Thus, the structures of the two residues closest to the lipophilic tail attachment were altered, but the key basic residues required for RyR activation (11–15) remained helical. Differences in the chemical shift patterns for ***A2(D-R18)*** and ***A2(D-R18)-2C$_{10}$*** are due to environmental changes caused by the attachment of the lipoamino acid tail to the N-terminus.

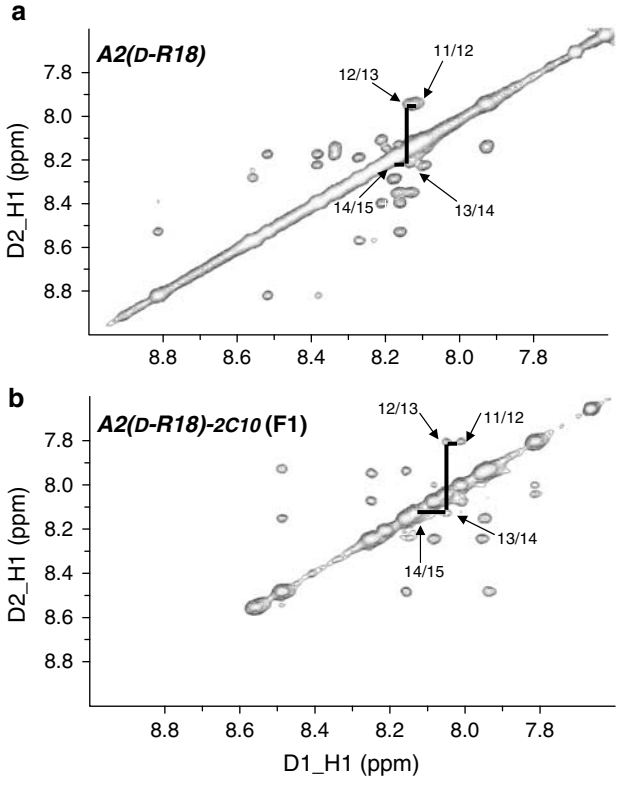

Figure 2 Conjugation of two -C10 lipid tails to ***A2(D-R18)*** does not significantly alter the helical structure of the peptide in the region of critical residues 11–15. Amide–amide regions of the NOESY spectra of peptides ***A2(D-R18)*** (a), and the active isomer of ***A2(D-R18)-2C10*** in HPLC fraction 1 (F1) (b). Connected $i+i-1$ NOEs are shown for residues 11–15 in (a, b). These residues are the RKRRK sequence, whose helical structure is required for optimal RyR activation. The spectra for both peptides indicate that they contain a substantial helical structure that includes residues 11–15.

The spectrum for the less active fraction 4 of ***A2(D-R18)-2C$_{10}$*** (not shown) had the same number of NOE cross-peaks as fraction 1, but interestingly residues 11–15 were not fully contained within the helix. The loss of helical structure of residues 11–15 is (a) consistent with the low activity of fraction 4 (see Methods and Results) and (b) showed that isomerisation at the junction between the peptide and the lipid could cause small changes in peptide structure away from the conjugation point.

In contrast to the peptides ***A2(D-R18)*** and Fraction 1 of ***A2(D-R18)-2C10***, ***A2(D-R18)-C12*** displayed an NOE cross-peak pattern indicative of a partial helical structure in the critical 11–15 amino-acid region (not shown). This may explain the reduced function of this peptide (Table 1), and is consistent with our hypothesis that this stretch of basic residues must be structurally ordered in a helical manner for optimal activation.

Lipoamino acid conjugation enhances the ability of peptides to release Ca^{2+} from SR

Ca^{2+} release from skeletal SR It was shown previously that mutating Ser 17 in the A1 peptide to an alanine (***A2*** peptide) increased its efficacy at inducing Ca^{2+} release from thapsigargin-blocked, skeletal SR (Casarotto *et al*., 2000). Furthermore, replacing the L isomer of Arg18 in ***A1*** by the D isomer, to give ***A1(D-R18)***, also increased the efficacy (Green *et al*., 2003) (e.g. see Figure 3). We show here that a peptide with both changes, ***A2(D-R18)***, is even more effective than the peptides with either change alone (Figure 4). Importantly, when ***A2(D-R18)*** was double conjugated with -C_{10}, to form ***A2(D-R18)-2C$_{10}$***, it became considerably more effective still, with the AC_{50} for resting Ca^{2+} release decreasing $\sim$5-fold to $\sim 3\,\mu$M and the maximum release rate more than doubling (Figure 4a). Furthermore, whereas ***A2(D-R18)*** did not evoke net release of Ca^{2+} in the absence of thapsigargin (Figure 3f), ***A2(D-R18)-2C$_{10}$*** did so (Figure 3g).

Fractionation of ***A2(D-R18)-2C$_{10}$*** yielded (a) an active isomer (fraction 1), which induced Ca^{2+} release with little intrinsic absorbance change (see Methods) and (b) a less active fraction 4, which had strong intrinsic effects. Resting Ca^{2+} release was similar for the racemic mixture and the active isomer at $\leqslant 20\,\mu$M (Figure 4a). The peptides also enhanced CICR and caffeine-induced Ca^{2+} release from the skeletal SR (Figure 4b). ***A2(D-R18)-2C$_{10}$*** was more active than ***A2(D-R18)*** and there was a further increase in activity with fraction 1.

Ca^{2+} release from cardiac SR Both conjugated and unconjugated peptides were active on cardiac SR, but their effects were small and in marked contrast to the large effect on skeletal SR. The unconjugated ***A2(D-R18)*** at 30 μM had little, if any, effect on the rate of release from the thapsigargin-treated cardiac vesicles (Figure 5a). Interestingly, double -C_{10} conjugation of the peptide greatly increased its ability to induce resting Ca^{2+} release, with fraction 1 of ***A2(D-R18)-2C$_{10}$*** apparently being more effective than the racemic mixture (Figure 5a). In contrast, similar lipoprotein conjugation of luteinising hormone-releasing hormone (LHRH), another small peptide with an unrelated sequence

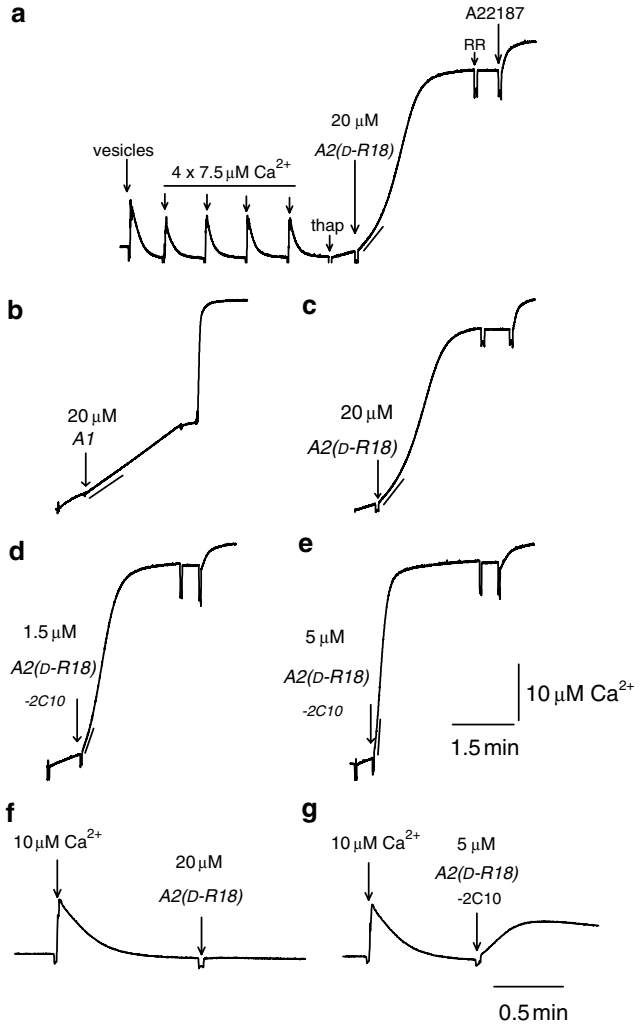

Figure 3 Conjugation of two -C10 lipid tails to ***A2(D-R18)*** enhances its ability to release Ca^{2+} from skeletal SR vesicles. (a) A full Ca^{2+} release experiment with addition of SR vesicles (first arrow), four additions of 7.5 μM Ca^{2+} with subsequent Ca^{2+} uptake into the SR (four short arrows). Thapsigargin addition to block the Ca^{2+}, Mg^{2+} ATPase (sixth arrow), followed by 20 μM ***A2(D-R18)*** (seventh arrow), ruthenium red (RR, eighth arrow) and the Ca^{2+} ionophore (A22187, ninth arrow). Release with 20 μM ***A1*** is shown in (b), 20 μM ***A1(D-R18)*** in (c) and 1.5 and 5.0 μM ***A2(D-R18)-2C10*** in (d, e), respectively. The line at the start of the Ca^{2+} release indicates the initial rate of release. Effects of the peptides in the absence of thapsigargin are shown in (f) (20 μM ***A2(D-R18)***) and (g) (5 μM ***A2(D-R18)-2C10***).

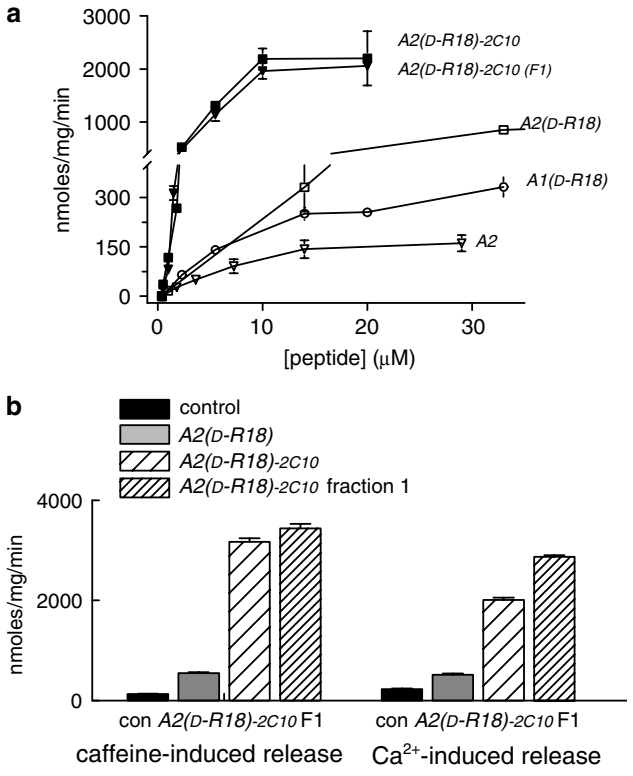

Figure 4 ***A2(D-R18)-2C10*** enhances resting Ca^{2+} release, caffeine-induced Ca^{2+} release and Ca^{2+}-induced Ca^{2+} release from isolated skeletal SR. Average data are shown for rates of resting Ca^{2+} release (a) and caffeine-induced Ca^{2+} release or Ca^{2+}-induced Ca^{2+} release in (b). Rates of release are given in nmol mg^{-1} min^{-1}. In (a), the vertical axis is split to display the rates of release with peptides ***A2*** ($n=10$), ***A1(D-R18)*** ($n=4$–6) and ***A2(D-R18)*** ($n=4$–6), as well as the greater rates of release with the racemic (unfractionated) ***A2(D-R18)-2C10*** ($n=7$–8) and the active isomer in fraction 1 (F1) of ***A2(D-R18)-2C10*** ($n=4$–6). In (b), average data for 0.76 mM caffeine-induced Ca^{2+} release (left) or 10 μM Ca^{2+}-induced Ca^{2+} release (right) under control conditions (control, $n=4$) and with 5 μM ***A2(D-R18)*** ($n=4$), the racemic ***A2(D-R18)-2C10*** ($n=4$) and fraction 1 (F1) of ***A2(D-R18)-2C10*** ($n=4$). Note that the low [caffeine] was used to obtain a slope that was low enough to see a clear effect of the peptide.

GHWSYTGLRPG-NH2, caused no increase in resting Ca^{2+} release (Figure 5a). The ***A1*** and ***A2*** peptides had a mild potentiating effect on CICR from cardiac SR vesicles and the effect of ***A2(D-R18)*** was similar (Table 1). In accord with the findings on resting Ca^{2+} release, double -C10 conjugation of ***A2(D-R18)*** enhanced its potentiating effect on CICR, with fraction 1 being even more efficacious with an AC_{50} of $\sim$1 μM (Figure 5b). Interestingly, single C_{12} conjugation of ***A2(D-R18)*** evidently interfered with the ability of the peptide to enhance CICR (Table 1).

In control experiments, Ca^{2+} release induced by the peptides was shown to depend on RyR channels and thapsigargin shown to block the Ca^{2+} ATPase (Figure 6). Ruthenium red blocked CICR (Figure 6a and b) and Ca^{2+} release induced with 1 μM ***A2(D-R18)-2C10*** (Figure 6c and d). [Ca^{2+}] did not fall after adding ruthenium red because Ca^{2+} pump activity was blocked by thapsigargin. A small residual release in ruthenium red was blocked by 10 mM Mg^{2+} (Figure 6f; 10 mM Mg^{2+} is a strong RyR antagonist – see skinned fibre results below). Similarly, Ca^{2+} release induced by 5 μM ***A2(D-R18)-2C10*** was fully blocked by ruthenium red (Figure 6e), with the OD measurement showing only the small artefactual change caused by the conjugated peptides (see Methods).

Lipoamino acid-conjugated peptides slow the rate of SR Ca^{2+} uptake Lipoamino acid conjugation exacerbated an effect of the peptides on the Ca^{2+} pump. In skeletal SR, Ca^{2+} accumulation was measured after adding 50 μM Ca^{2+} to the cuvette (Figure 7a). The decline in [Ca^{2+}] (slope A, Figure 7a) reflected the net Ca^{2+} flux (uptake by the pump minus the efflux through the RyR). ***A2(D-R18)-2C$_{10}$*** was more effective

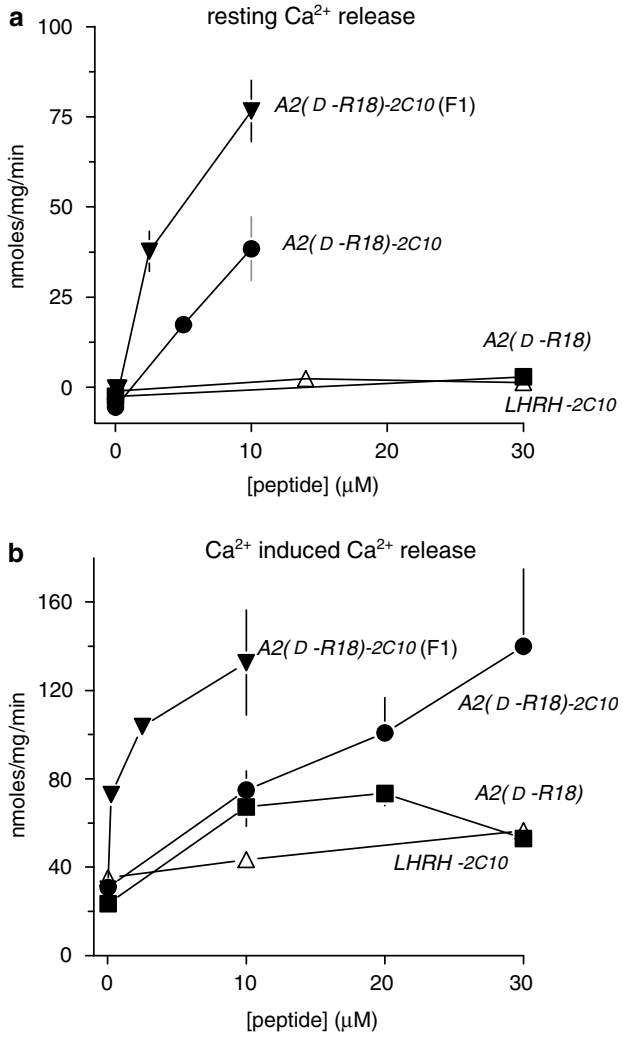

Figure 5 ***A2(D-R18)-2C10*** enhances resting Ca^{2+} release and Ca^{2+}-induced Ca^{2+} release from isolated cardiac SR. Average rates of resting Ca^{2+} release (RCR) are shown in (a) and Ca^{2+}-induced Ca^{2+} release (CICR) in (b). In (a, b), data are shown for ***A2(D-R18)*** (RCR – $n=2$; CICR – $n=6$–9), the racemic ***A2(D-R18)-2C$_{10}$*** (RCR – $n=4$; CICR – $n=3$) and fraction 1 (F1) of ***A2(D-R18)-2C$_{10}$*** (RCR – $n=5$–7; CICR – $n=3$–4) and for a control peptide (***LHRH***) with two -C10 tails (***LHRH-2C$_{10}$***) ($n=2$ each for RCR and CICR). Note, in panel b that there is some CICR even in the absence of any peptide.

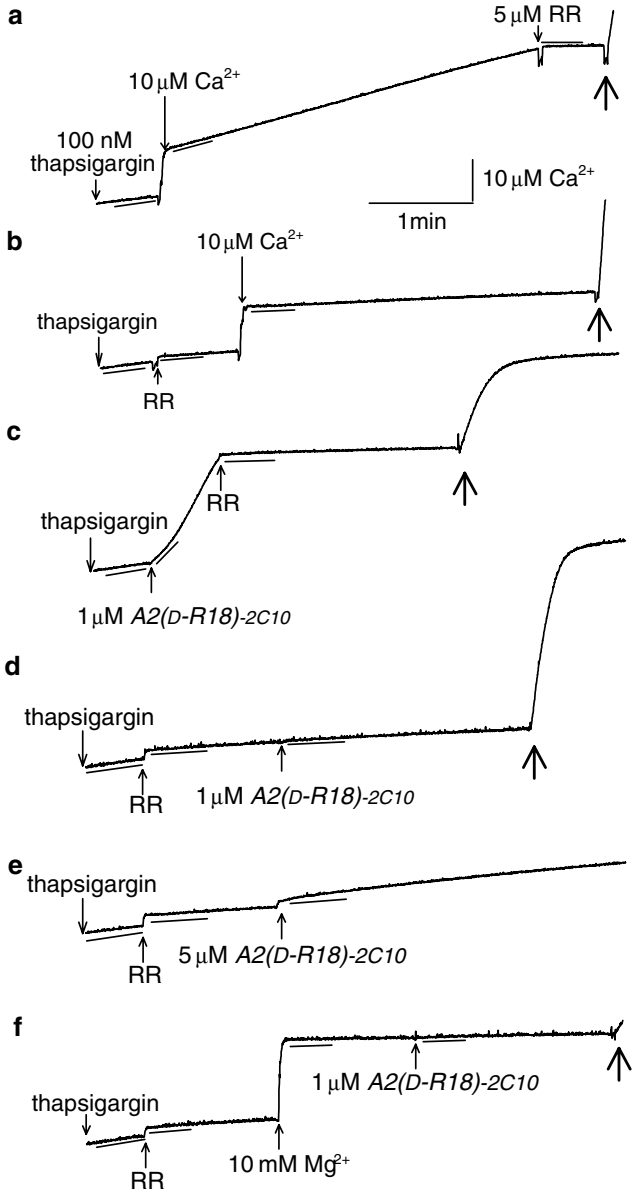

Figure 6 Control experiments showing that Ca^{2+} release is through the RyR and that the Ca^{2+} pump is blocked by thapsigargin. Records show Ca^{2+} release from skeletal SR. Vesicles were loaded with $4\times7.5\,\mu$M Ca^{2+} (as in Figure 3a) and 100 nM thapsigargin added as indicated. In (a), release in response to 10 μM Ca^{2+} was blocked by 5 μM ruthenium red. In (b), 5 μM ruthenium red added after 100 nM thapsigargin reduced the Ca^{2+} leak and prevented the CICR response. In (c), release with 1 μM ***A2(D-R18)-2C$_{10}$*** was blocked by 5 μM ruthenium red. In (d, e) ruthenium red added before 1 or 5 μM peptide, respectively, prevented release. In (f), 10 mM Mg^{2+} (added after ruthenium red block) caused a step increase in optical density, but abolished residual release and the peptide-induced response. The maintained high [Ca^{2+}] after adding ruthenium red in (a–c) indicates that the Ca^{2+}, Mg^{2+} ATPase was blocked by thapsigargin. The heavy arrow towards the end of records in (a–d, f) indicates the time of addition of Ca^{2+} ionophore A23187 (3 μg ml^{-1}) to release the Ca^{2+} remaining in the TC vesicles.

than the unconjugated ***A2(D-R18)*** in reducing Ca^{2+} accumulation (Figure 7b) – consistent with their relative effects on Ca^{2+} efflux. After adding ruthenium red, accumulation (slopes B and C, Figure 7) reflected Ca^{2+} uptake alone and was reduced minimally by 25 μM ***A2(D-R18)*** (second column), and reduced further by 5–10 μM ***A2(D-R18)-2C$_{10}$***. Notably, the decrease in Ca^{2+} uptake rate with 5 μM of the -*2C$_{10}$* conjugated peptide to 0.8–0.5 of control is in contrast to the 10,000-fold increase in resting Ca^{2+} release rate with the same peptide concentration (see Figure 4 above).

The protocol was altered with cardiac SR because the SR failed to accumulate 50 μM Ca^{2+}, but coped with a smaller pulse of 7.5 μM Ca^{2+} (Figure 8a and b). The effect of ruthenium red was small (Figure 8), indicating that the leak through the RyR was only small, most likely due to (a) there being excess longitudinal SR (which lacks RyRs), since the cardiac preparation was not fractionated by sucrose gradient (see Methods) and (b) low loading with addition of only 7.5 μM Ca^{2+}. Thus, Ca^{2+} accumulation was dominated by Ca^{2+} uptake, even in the absence of ruthenium red. ***A2(D-R18)*** did not alter Ca^{2+} accumulation, nor did unconjugated ***A1*** nor ***A2***

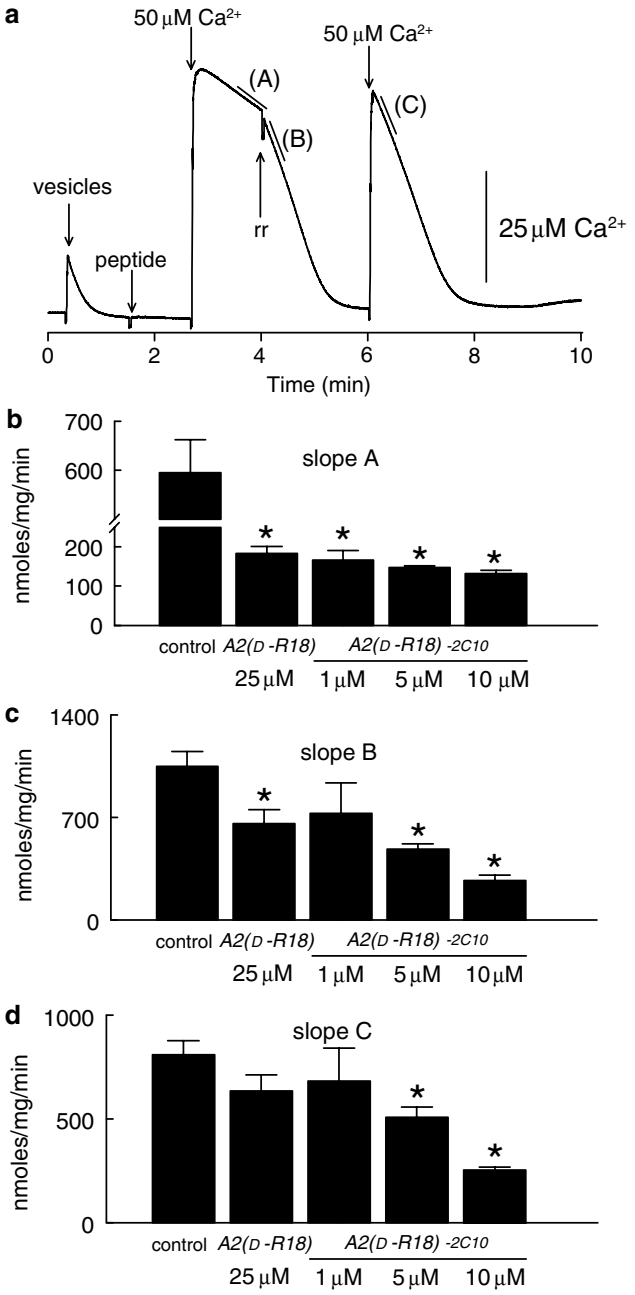

Figure 7 ***A2(D-R18)-2C10*** reduces Ca^{2+} accumulation by skeletal SR by increasing Ca^{2+} efflux through the RyR and by reducing Ca^{2+} uptake by the Ca^{2+}, Mg^{2+} ATPase. (a) A record showing skeletal SR vesicles added to the cuvette (first arrow), followed by either H_2O (control) or peptide (second arrow). Ca^{2+} accumulation measured ~30 s after adding 50 μM Ca^{2+} (third arrow) (line A), and then after addition of ruthenium red (fourth arrow) to block the RyR (line B). When extravesicular Ca^{2+} was reduced to resting levels, a second bolus 50 μM Ca^{2+} was added (fifth arrow) and Ca^{2+} uptake measured (line C). The rate of accumulation after addition of ruthenium red (slopes B and C) reflected Ca^{2+} uptake by the Ca^{2+}, Mg^{2+} ATPase. Average data corresponding to slopes A, B and C are given in (b–d), respectively. The first bin in each graph shows control data (with the volume of H_2O normally added with 25 μM peptide). The second bin shows data with 25 μM ***A2(D-R18)***, while the third, fourth and fifth bins show data with 1, 5 and 10 μM ***A2(D-R18)-2C10***, respectively. Each bin gives mean ± s.d. for three observations. Asterisks indicate a significant difference from control.

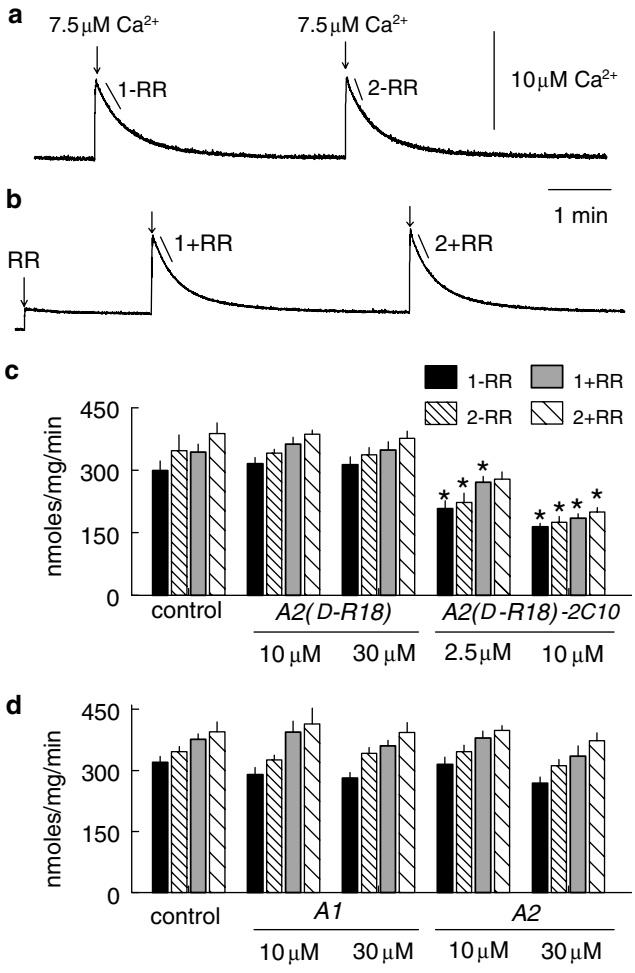

Figure 8 ***A2(D-R18)-2C10*** inhibits Ca^{2+} uptake by the cardiac Ca^{2+},Mg^{2+} ATPase. (a, b) Records of a pair of experiments with cardiac SR vesicles. Either water (control) or peptide was added (not shown). Ca^{2+} accumulation was measured after each of two additions of 7.5 μM Ca^{2+} (lines 1 and 2, respectively) – (a) in the absence of ruthenium red (−RR); (b) ruthenium red added before Ca^{2+} (+RR). (c, d) Average data under control conditions (with the volume of H_2O added with 30 μM peptide) and in the presence of the peptides. Four bins are shown under each condition: slope 1−RR (1−RR), slope 2−RR (2−RR), slope 1+RR (1+RR) and slope 2+RR (2+RR). The legend in (c) also applies to (d). The influence of RyR activity on uptake, that is, uptake in the presence and absence of RyR activity can be assessed by comparing the black (1−RR) with the grey filled bins (1+RR) or the narrow (2−RR) with the wide stippled bins (2+RR). (c) ***A2(D-R18)*** at 10 and 30 μM ($n=5$), and Fraction 1 of ***A2(D-R18)-2C10*** at 2.5 and 10 μM ($n=5$–7). (d) ***A1*** and ***A2*** at 10 and 30 μM ($n=5$ for each).

(Figure 8c and d). In contrast, the racemic ***A2(D-R18)-2C$_{10}$*** at 2.5 μM slowed the decline in [Ca^{2+}] under all conditions to ~0.8 of control. These effects were consistent with (a) a minimal influence of Ca^{2+} efflux on the measurements and (b) inhibition of the pump by ***A2(D-R18)-2C$_{10}$***.

Effects of lipoamino acid-conjugated peptides on skinned skeletal muscle fibres

The unconjugated ***A2(D-R18)*** potentiated caffeine-induced Ca^{2+} release in skinned EDL fibres. The peptide was more effective than ***A1(D-R18)*** (Green *et al*., 2003), with 0.6 μM peptide increasing both the amplitude and rate of Ca^{2+} release

Table 2 Effect of peptides on the force response to 8 mM caffeine in rat skinned EDL fibres

	Peak response to 8 mM caffeine (% of maximum Ca^{2+}-activated force)			*Rate of force rise to 8 mM caffeine (% Ca^{2+}-activated maximum force per sec)*		
	Control	*Test 1*	*Test 2*	*Control*	*Test 1*	*Test 2*
A2(D-R18) (0.6 μM) ($n=7$)	19±5.6	51±5.6*	58±10.2*	6±1.8	25±6.5*	32±7.0*
A2(D-R18) (3 μM) ($n=4$)	31±9.6	79±10*	77±5.4*	9±3.6	74±20*	70±15*
A2(D-R18)-2C10 (0.6 μM) ($n=5$)	22±12	37±12*	52±9.1*	12±8.0	16±6.2	21±6.6
A2(D-R18)-2C10 (3 μM) ($n=3$)	35±9.3	59±21	44±20	12±3.2	29±13.7	23±10.2
A2(D-R18)-2C10 (10 μM) ($n=3$)	15±15	74±12.3*	84±7.5*	2±1.6	23±7.5*	34±8.5*

In each skinned fibre, the force response to 8 mM caffeine was measured twice in the absence of peptide (and averaged) and then twice in the presence of the peptide (tests 1 and 2) (see Figure 9), and expressed as a percentage of the maximum Ca^{2+}-activated force in that fibre. The table shows the mean±s.e.m. data obtained in the indicated number of fibres (n). Note that, although the size of control response to 8 mM caffeine could differ somewhat between fibres, it was highly reproducible within a given fibre (e.g. Figure 9), and that paired control and test data were always obtained in each fibre.
*Significant difference ($P<0.05$) between control and test response (Student's one-tailed paired t-test).

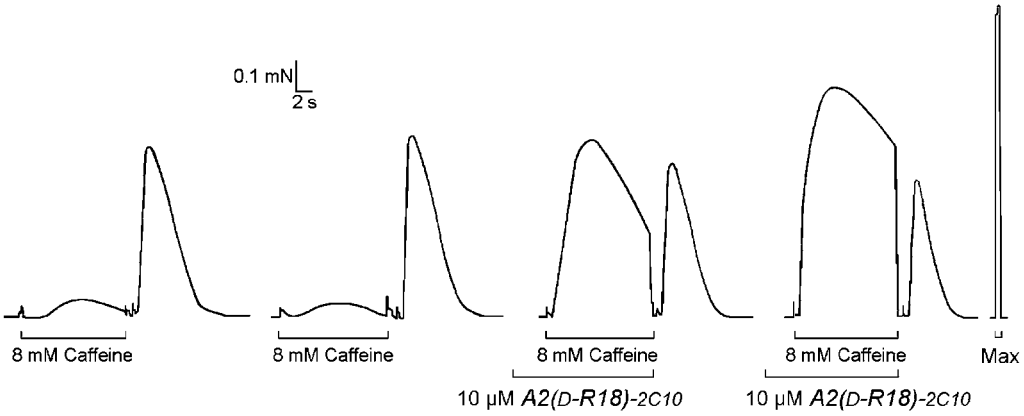

Figure 9 ***A2(D-R18)-2C10*** potentiates caffeine-induced Ca^{2+} release in a skinned EDL fibre. A skinned EDL fibre was subjected to repeated cycles in which the SR was emptied of all Ca^{2+} and then reloaded to a set level and the responsiveness to 8 mM caffeine tested. The response to 8 mM caffeine was greatly potentiated by 10 μM ***A2(D-R18)-2C10***. After testing the response to 8 mM caffeine, the SR was depleted of its remaining Ca^{2+} by exposure to the Full Release Solution, with the area of the resulting force response being indicative of the amount of Ca^{2+} that was in the SR. When 8 mM caffeine elicited a bigger force response, and hence more Ca^{2+} release, the amount of Ca^{2+} left in the SR decreased. Note that the 'area' of the force response to 8 mM caffeine cannot be directly compared to that when fully releasing the Ca^{2+} because of the very different levels of Ca^{2+} buffering in the two cases. The peptide was added 20 s before testing the responsiveness to 8 mM caffeine. 'Max' indicates maximum Ca^{2+}-activated force for the fibre.

(Table 2). This effect of the peptide was substantially reversed within 2 min after washout of the peptide (not shown).

A2(D-R18)-2C$_{10}$ also potentiated caffeine-induced responses (Figure 9), with a significant increase in amplitude at 0.6 μM and a significant effect on rate at 10 μM (Table 2). In contrast to Ca^{2+} release from isolated SR (Figures 3 and 4), conjugation seemingly reduced the relative effectiveness of the peptide in skinned fibres. However, this was almost certainly because the strong partitioning of the hydrophobic peptide into the membranes meant that the 20 s period allowed for full equilibration with the RyR was insufficient. (The 20 s equilibration period could not be increased because the peptide was likely to cause too great a loss of Ca^{2+} from the SR before the exposure to 8 mM caffeine.) Strong partitioning into the membrane was further indicated by the fact that the effect of ***A2(D-R18)-2C$_{10}$*** on the caffeine response was only partially reversed after >10 min washout. Thus, the observed effects of ***A2(D-R18)-2C$_{10}$*** on caffeine-induced Ca^{2+} release almost certainly underestimate its efficacy.

The enhancement of caffeine responses by ***A2(D-R18)-2C$_{10}$*** was evidently due to an effect on Ca^{2+} release from the SR, not on the Ca^{2+} sensitivity of the contractile apparatus. Firstly, the force response when emptying the SR of its remaining Ca^{2+} after exposure to 8 mM caffeine was smaller when peptide had been present in the 8 mM caffeine solution (Figure 9). Such a reduced response indicates that the presence of the peptide in the 8 mM caffeine solution caused greater depletion of Ca^{2+} in the SR. Secondly, direct examination of the contractile apparatus showed that ***A2(D-R18)-2C$_{10}$*** (at 3 μM) had no effect on maximum force or Ca^{2+} sensitivity (pCa_{50} and Hill coefficient: 5.96±0.01 and 4.4±0.6, and 5.96±0.01 and 4.2±0.7, with and without peptide, respectively; $P>0.05$, Student's paired t-test, $n=4$).

A2(D-R18)-2C$_{10}$ substantially inhibited net Ca^{2+} accumulation by the SR (Figure 10a). In these experiments, where the SR was initially empty of Ca^{2+}, it was possible to equilibrate the fibres with peptide for 1 min before testing its effect on Ca^{2+} accumulation. The effect of the conjugated peptide on Ca^{2+} accumulation became greater with repetition (stabilising after ~3 repetitions), consistent with a slow time-course for full equilibration of the peptide within the fibre. ***A2(D-R18)-2C$_{10}$*** (10 μM) reduced the net uptake rate to 18±4% of control

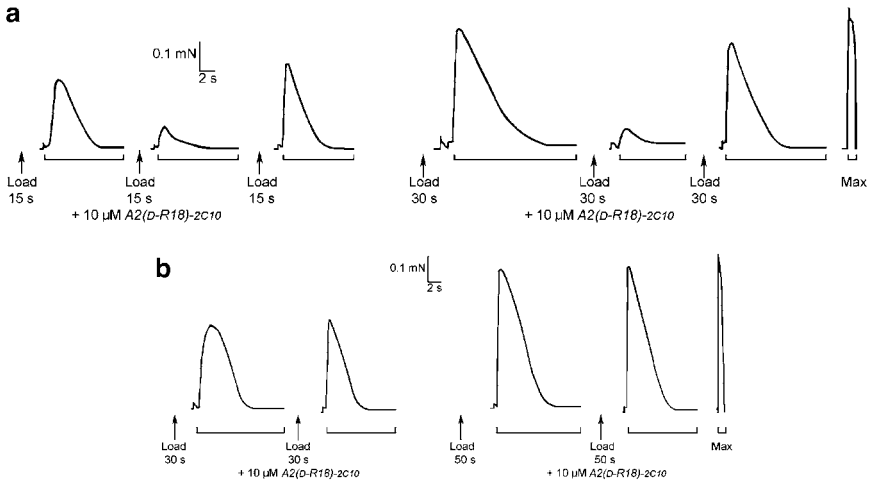

Figure 10 Peptide ***A2(D-R18)-2C10*** reduces net Ca^{2+} uptake by the SR in a skinned EDL fibre when present in the loading solution. In (a), force responses were elicited when emptying the SR with the Full Release Solution after loading for the indicated time, under the standard conditions with 1 mM Mg^{2+} (pCa 6.7, 1 mM total EGTA), with or without peptide. The area of the force response is indicative of the net amount of Ca^{2+} loaded into the SR. The peptide reduced net Ca^{2+} uptake and the effect became greater on successive repetitions (stabilising after $\sim$3 repetitions) and was reversed only slowly by washout. The records shown are for the third repetition after loading in the presence of the peptide, and the following control records are for the fourth load/release cycle after washout of the peptide. In the fibre shown in (b), ***A2(D-R18)-2C10*** caused only a small reduction in net SR Ca^{2+} uptake when there was 10 mM free Mg^{2+} in the loading solution. The reduced effect of the peptide was due to the high [Mg^{2+}] inhibiting activation of the Ca^{2+} release channels and preventing the peptide from increasing Ca^{2+} efflux from the SR during uptake. These findings indicate that most of the reduction in net Ca^{2+} uptake by the peptide in (a) is due to increased Ca^{2+} efflux, not reduced uptake. (Note that the rate of Ca^{2+} uptake is reduced in 10 mM Mg^{2+} but this effect was minimised by raising the [Ca^{2+}] in the load solution from pCa 6.7 to 6.4, so that the net Ca^{2+} loaded into the SR is comparable with that in (a)). In (a, b) Ca^{2+} release was evoked under the standard conditions with 1 mM Mg^{2+}.

(on the third repetition in peptide) ($n=6$ fibres). The effect was slowly reversed by washout (taking $\sim$10 min for near full recovery, legend to Figure 10). The effect of the peptide in reducing net Ca^{2+} accumulation was consistent with it enhancing Ca^{2+} efflux through the RyR during the Ca^{2+}-loading period. The greater effect with successive repetitions and slow washout are consistent with retarded equilibration of the peptide at its active site.

The possibility that the conjugated peptide also slowed Ca^{2+} uptake by the Ca^{2+} pump was examined by blocking Ca^{2+} efflux with 10 mM free Mg^{2+} – a potent inhibitor of the RyR (Lamb & Stephenson, 1994). Under such circumstances, 10 μM of ***A2(D-R18)-2C$_{10}$*** reduced net uptake to only 71$\pm$8% of control ($n=6$ fibres, $P<0.05$) (e.g. Figure 10b). The fact that uptake still declined when the RyR was disabled indicates that the peptide directly inhibits the SR Ca^{2+} pump. Nevertheless, it is apparent that most of the reduction in net Ca^{2+} accumulation observed at normal [Mg^{2+}] (e.g. Figure 10a) was due to the peptide potentiating the Ca^{2+} efflux from the SR during Ca^{2+} loading. These results are in close accord with those found in the skeletal SR vesicles.

Discussion

We find that peptides, with sequences based on the ***A*** region of the skeletal muscle DHPR II–III loop, become permeable in a Caco-2 cell line assay following lipoamino acid conjugation. Importantly, the conjugation did not significantly alter the α-helical structure of residues that are critical for high-affinity activation of RyR Ca^{2+} channels, and did not interfere with the ability of the peptides to release Ca^{2+} from the SR. In fact, the conjugation increased the efficacy of the peptides in inducing Ca^{2+} release from both skeletal and cardiac SR.

Permeability of lipoamino acid-conjugated peptides

As shown previously with other peptides (Wong *et al*., 2002), the lipoamino acid conjugation enhanced the ability of the poorly absorbed native peptides to cross the epithelial cell layer. In order for a compound to be well absorbed, it should have an apparent permeability in Caco-2 monolayers of $\sim 1\times10^{-6}$ cm s^{-1} (Artursson & Karlsson, 1991). Since ***A2(D-R18)-C10*** had a P_{app} value of 0.97×10^{-6}, it should be well absorbed *in vivo*. Passive transport pathways across the epithelium are through tight junctions and across the apical and basolateral cell membranes (Artursson *et al*., 2001; Wong *et al*., 2002). The poorly permeable hydrophilic ***A2(D-R18)*** probably diffused through tight junctions, which provide the usual route for water-soluble compounds. The enhanced permeability of the hydrophobic lipoamino acid conjugates suggested that they crossed the cell membranes. The low apparent permeability of the more hydrophobic ***A2(D-R18)-2C$_{10}$*** (compared with ***A2(D-R18)-C$_{10}$***), can be explained by a lower than expected [peptide] in the donor solution, due to lower solubility and tendency to adsorb onto the chamber wall. High adsorbance can reduce apparent permeability by at least an order of magnitude (Artursson & Karlsson, 1991).

Structure of the conjugated peptides

The ability of the ***A*** peptides to stimulate Ca^{2+} release through the RyR depends on the presence of a stretch of positively charged amino-acid residues along one surface of the α-helical

peptide (Casarotto *et al*., 2000; 2001; Green *et al*., 2003). The profile of the NOESY spectra provides sufficient information to assess the integrity of secondary structure without performing a full structural analysis. The NOE cross-peak pattern in the amide region showed that the helical nature of the peptides was essentially retained despite the modification of the N-terminus by the lipoamino acid attachment. In particular, it was shown that the involvement of a helix for residues 11–15 was still a requirement in order for these peptides to release Ca^{2+} from the SR. This point was clearly evident for the two fractions of ***A2(D-R18)-2C$_{10}$*** where the stereochemistry related to the lipophilic attachment influenced the structure of the peptide portion and hence the functional response of the peptide. Thus, functional changes in the conjugated peptides can be attributed to the increased hydrophobicity of the peptide, rather than altered peptide structure.

RyR activation by lipoamino acid-conjugated peptides

The lipoamino acid conjugation of ***A2(D-R18)*** considerably enhanced its ability to release Ca^{2+} from isolated SR. Since the control ***LHRH-2C$_{10}$*** peptide did not release Ca^{2+} or enhance CICR, the lipoamino acid tails *per se* did not contribute to Ca^{2+} release.

Different actions of the peptides on skeletal and cardiac SR

The effects of the A peptides on skeletal SR were significantly stronger than the effects on cardiac SR. The lower sensitivity of the cardiac preparation presumably reflects differences between the binding sites or in the environment of the binding site in different RyR isoforms. A further reflection of possible differences in the environment of the binding site is the fact that the active fraction 1 (F1) of ***A2(D-R18)-2C$_{10}$*** was as effective as the racemic ***A2(D-R18)-2C$_{10}$*** in releasing Ca^{2+} in the skeletal preparation, but was substantially more effective in the cardiac preparation (although its effect remained far less than that on skeletal SR).

Slow equilibration of lipoamino acid-conjugated peptides in skinned fibres

In contrast to the greater efficacy of the lipoamino acid-conjugated peptides in releasing Ca^{2+} from isolated SR, ***A2(D-R18)-C$_{10}$*** was less effective in enhancing caffeine-induced Ca^{2+} release in skinned fibres when equilibration times were brief ($\sim$20 s). However, when the preparation was successively exposed to ***A2(D-R18)-C$_{10}$*** (with 1 min equilibration during each exposure), a progressively greater effect on Ca^{2+} accumulation was observed, which was attributed to enhanced Ca^{2+} efflux. This indicated that equilibration of the conjugated peptide at its active site was slower than accumulation of the unconjugated peptide. Slow equilibration is consistent with the hydrophobic peptide partitioning into the lipid of the t-tubule and SR membranes that surround the RyR and form two boundaries of the restricted space of the triad junction (Franzini-Armstrong, 1970), as seen in the skinned fibres with other lipid-permeable agents such as nifedipine (Posterino & Lamb, 1998). It is also evidence that the conjugated peptides readily permeate the cell membranes of muscle fibres.

Lipoamino acid conjugation of the A *peptides reveals an action on the Ca^{2+} pump*

A small and low-affinity effect of the conjugated ***A*** peptides on the Ca^{2+}, Mg^{2+} ATPase was apparent. Since fast-twitch skeletal and cardiac SR contain different isoforms of SR, endoplasmic reticulum Ca^{2+} ATPase (SERCA), SERCA1 and SERCA2a, respectively (MacLennan *et al*., 1997), the effect is not isoform specific. A small decline in Ca^{2+} uptake by skeletal SR exposed to the unconjugated ***A2(D-R18)*** suggested that the hydrophilic peptide may have restricted access to an inhibitory site located in a hydrophobic region of the protein.

Potential use for lipoamino acid-conjugated A *peptides*

Within a limited concentration range, ***A2(D-R18)-2C$_{10}$*** is a specific activator of the skeletal RyR in SR vesicles and skinned fibres. ***A2(D-R18)-2C$_{10}$*** at 2 μM produced an $\sim$2000-fold increase in Ca^{2+} release from skeletal SR without affecting the Ca^{2+} pump. At higher concentrations where small effects on the cardiac RyR and on Ca^{2+} uptake by the Ca^{2+}, Mg^{2+} ATPase were apparent, the activation of RyR1 was several orders of magnitude greater than the effects on RyR2 or the SERCA proteins. The peptide at 20 μM caused a 20,000-fold increase in Ca^{2+} release from skeletal SR, compared with only a four-fold reduction in Ca^{2+} uptake. The peptide enhanced caffeine-induced Ca^{2+} release in skinned fibres at 0.6 μM, and at 10 μM increased caffeine-induced Ca^{2+} release $\sim$6-fold with only a 30% decline in pump activity. Therefore, ***A2(D-R18)-2C$_{10}$*** is a membrane-permeable peptide that selectively activates Ca^{2+} release from skeletal SR through RyR channels at concentrations $\leqslant$2 μM.

In conclusion, the experiments show that lipoamino acid conjugation renders the ***A*** peptides membrane permeable, without significantly altering either the α-helical secondary structure of a critical region of the peptides or altering their ability to stimulate RyR activity. The present study constitutes proof of principal that lipoamino acid conjugation of ***A*** peptides is a potentially promising method for developing membrane-permeable specific stimulators of RyRs for use *in vivo*.

We are grateful to Joan Stivala for assistance with SR vesicle preparation and characterisation and Maria Cellini for help with the skinned fibre experiments. This work was supported by Australian NHMRC Project Grant #224237 and the National Heart Foundation of Australian (# G 01C 0296).

References

AHERN, C.A., BHATTACHARYA, D., MORTENSON, L. & CORONADO, R. (2001). A component of excitation–contraction coupling triggered in the absence of the T671-L690 and L720-Q765 regions of the II–III loop of the dihydropyridine receptor alpha (1 s) pore subunit. *Biophys. J.,* **81,** 3294–3307.

AHERN, G.P., JUNANKAR, P.R. & DULHUNTY, A.F. (1994). Single channel activity of the ryanodine receptor calcium release channel is modulated by FK-506. *FEBS Lett.,* **352,** 369–374.

ARTURSSON, P. & KARLSSON, J. (1991). Correlation between oral drug absorption in humans and apparent drug permeability coefficients in human intestinal epithelial (Caco-2) cells. *Biochem. Biophys. Res. Commun.,* **175,** 880–885.

ARTURSSON, P., KARLSSON, J., OCKLIND, G., SCHIPPER, N. & KARLSSON, J. (1996). Studying transport processes in absorptive epithelia. In: *Epithelial Cell Culture: A Practical Approach,* ed. Shaw, A.J. pp. 111–129. Oxford, England: IRL Press.

ARTURSSON, P., PALM, K. & LUTHMAN, K. (2001). Caco-2 monolayers in experimental and theoretical predictions of drug transport. *Adv. Drug Deliv. Rev.,* **46,** 27–43.

BAX, A. & DAVIS, D.G. (1985). MLEV-17 based two dimensional homonuclear magnetisation transfer spectroscopy. *J. Magn. Reson.,* **65,** 355–360.

BLOCK, B.A., IMAGAWA, T., CAMPBELL, K.P. & FRANZINI-ARMSTRONG, C. (1988). Structural evidence for direct interaction between the molecular components of the transverse tubule/sarcoplasmic reticulum junction in skeletal muscle. *J. Cell Biol.,* **107,** 2587–2600.

CASAROTTO, M.G., GREEN, D., PACE, S.M., CURTIS, S.M. & DULHUNTY, A.F. (2001). Structural determinants for activation or inhibition of ryanodine receptors by basic residues in the dihydropyridine receptor II–III loop. *Biophys. J.,* **80,** 2715–2726.

CASAROTTO, M.G., GIBSON, F., PACE, S.M., CURTIS, S.M., MULCAIR, M. & DULHUNTY, A.F. (2000). A structural requirement for activation of skeletal ryanodine receptors by peptides of the dihydropyridine receptor II–III loop. *J. Biol. Chem.,* **275,** 11631–11637.

CHAMBERLAIN, B.K. & FLEISCHER, S. (1988). Isolation of canine cardiac sarcoplasmic reticulum. *Methods Enzymol.,* **157,** 91–99.

DULHUNTY, A.F., HAARMANN, C.S., GREEN, D., LAVER, D.R., BOARD, P.G. & CASAROTTO, M.G. (2002). Interactions between dihydropyridine receptors and ryanodine receptors in striated muscle. *Prog. Biophys. Mol. Biol.,* **79,** 45–75.

DULHUNTY, A.F., LAVER, D.R., GALLANT, E.M., CASAROTTO, M.G., PACE, S.M. & CURTIS, S. (1999). Activation and inhibition of skeletal RyR channels by a part of the skeletal DHPR II–III loop: effects of DHPR Ser687 and FKBP12. *Biophys. J.,* **77,** 189–203.

EL-HAYEK, R., ANTONIU, B., WANG, J., HAMILTON, S.L. & IKEMOTO, N. (1995). Identification of calcium release-triggering and blocking regions of the II–III loop of the skeletal muscle dihydropyridine receptor. *J. Biol. Chem.,* **270,** 22116–22118.

FRANZINI-ARMSTRONG, C. (1970). Studies of the triad. I. Structure of the junction in frog twitch fibers. *J. Cell Biol.,* **47,** 488–498.

GIBBONS, W.A., HUGHES, R.A., SZETO, A., CHARALAMBOUS, M., AULABAUGH, A., PAOLO MASCAGNI, P. & TOTH, I. (1990). Lipidic peptides I. Synthesis resolution and structural elucidation of fatty amino acids and their homo- and hetero-oligomers. *Liebigs Ann. Chem.,* 1175–1183.

GREEN, D., PACE, S., CURTIS, S.M., SAKOWSKA, M., LAMB, G.D., DULHUNTY, A.F. & CASAROTTO, M.G. (2003). The three-dimensional structural surface of two beta-sheet scorpion toxins mimics that of an alpha-helical dihydropyridine receptor segment. *Biochem. J.,* **370,** 517–527.

GURROLA, G.B., AREVALO, C., SREEKUMAR, R., LOKUTA, A.J., WALKER, J.W. & VALDIVIA, H.H. (1999). Activation of ryanodine receptors by imperatoxin A and a peptide segment of the II–III loop of the dihydropyridine receptor. *J. Biol. Chem.,* **274,** 7879–7886.

INGELS, F., DEFERME, S., DESTEXHE, E., OTH, M., VAN DEN MOOTER, G. & AUGUSTIJNS, P. (2002). Simulated intestinal fluid as transport medium in the Caco-2 cell culture model. *Int. J. Pharm.,* **232,** 183–192.

KUMAR, A., ERNST, R.R. & WUTHRICH, K. (1980). A two-dimensional nuclear overhauser enhancement (2D nOe) experiment for the elucidation of complete proton–proton cross-relaxation networks in biological molecules. *Biochem. Biophys. Res. Commun.,* **95,** 1–6.

LAMB, G.D., CELLINI, M.A. & STEPHENSON, D.G. (2001). Different Ca^{2+} releasing action of caffeine and depolarisation in skeletal muscle fibres of the rat. *J. Physiol.,* **531,** 715–728.

LAMB, G.D., EL-HAYEK, R., IKEMOTO, N. & STEPHENSON, D.G. (2000). Effects of dihydropyridine receptor II–III loop peptides on Ca^{2+} release in skinned skeletal muscle fibers. *Am. J. Physiol. Cell Physiol.,* **279,** C891–C905.

LAMB, G.D. & STEPHENSON, D.G. (1994). Effects of intracellular pH and $[Mg^{++}]$ on excitation–contraction coupling in skeletal muscle fibres of the rat. *J. Physiol.,* **478,** 331–339.

LAVER, D.R., RODEN, L.D., AHERN, G.P., EAGER, K.R., JUNANKAR, P.R. & DULHUNTY, A.F. (1995). Cytoplasmic Ca^{2+} inhibits the ryanodine receptor from cardiac muscle. *J. Membr. Biol.,* **147,** 7–22.

MACLENNAN, D.H., RICE, W.J. & GREEN, N.M. (1997). The mechanism of Ca^{2+} transport by sarco(endo)plasmic reticulum Ca^{2+}-ATPases. *J. Biol. Chem.,* **272,** 28815–28818.

MOSBAH, A., KHARRAT, R., FAJLOUN, Z., RENISIO, J.G., BLANC, E., SABATIER, J.M., EL AYEB, M. & DARBON, H. (2000). A new fold in the scorpion toxin family, associated with an activity on a ryanodine-sensitive calcium channel. *Proteins,* **40,** 436–442.

POSTERINO, G.S. & LAMB, G.D. (1998). Effect of nifedipine on depolarization-induced force responses in skinned skeletal muscle fibres of rat and toad. *J. Muscle Res. Cell Motil.,* **19,** 53–65.

PROENZA, C., WILKENS, C.M. & BEAM, K.G. (2000). Excitation–contraction coupling is not affected by scrambled sequence in residues 681–690 of the dihydropyridine receptor II–III loop. *J. Biol. Chem.,* **275,** 29935–29937.

SAGARA, Y. & INESI, G. (1991). Inhibition of the sarcoplasmic reticulum Ca^{++} transport ATPase by thapsigargin at subnanomolar concentrations. *J. Biol. Chem.,* **266,** 13503–13506.

STANGE, M., TRIPATHY, A. & MEISSNER, G. (2001). Two domains in dihydropyridine receptor activate the skeletal muscle Ca(2+) release channel. *Biophys. J.,* **81,** 1419–1429.

TANABE, T., BEAM, K.G., POWELL, J.A. & NUMA, S. (1988). Restoration of excitation–contraction coupling and slow calcium current in dysgenic muscle by dihydropyridine receptor complementary DNA. *Nature,* **336,** 134–139.

TOTH, I., & KERI, G. (2003). *Molecular Pathomechanisms and New Trends in Drug Research*. London and New York: Taylor & Francis.

TOTH, I., MALKINSON, J.P., FLINN, N.S., DROUILLAT, B., HORVATH, A., ERCHEGYI, J., IDEI, M., VENETIANER, A., ARTURSSON, P., LAZOROVA, L., SZENDE, B. & KERI, G. (1999). Novel lipoamino acid- and liposaccharide-based system for peptide delivery: application for oral administration of tumor-selective somatostatin analogues. *J. Med. Chem.,* **42,** 4010–4013.

TRIPATHY, A., RESCH, W., XU, L., VALDIVIA, H.H. & MEISSNER, G. (1998). Imperatoxin A induces subconductance states in Ca^{2+} release channels (ryanodine receptors) of cardiac and skeletal muscle. *J. Gen. Physiol.,* **111,** 679–690.

WILKENS, C.M., KASIELKE, N., FLUCHER, B.E., BEAM, K.G. & GRABNER, M. (2001). Excitation–contraction coupling is unaffected by drastic alteration of the sequence surrounding residues L720–L764 of the alpha 1S II–III loop. *Proc. Natl. Acad. Sci. U.S.A.,* **98,** 5892–5897.

WONG, A.K., ROSS, B.P., CHAN, Y.N., ARTURSSON, P., LAZOROVA, L., JONES, A. & TOTH, I. (2002). Determination of transport in the Caco-2 cell assay of compounds varying in lipophilicity using LC–MS: enhanced transport of Leu-enkephalin analogues. *Eur. J. Pharm. Sci.,* **16,** 113–118.

(Received June 1, 2004
Revised July 30, 2004
Accepted August 23, 2004)